Measurement of the $^{13}C(\alpha, n_0)^{16}O$ Differential Cross Section from 0.8 to 6.5 MeV

R. J. deBoer,[1,*] M. Febbraro,[2] D. W. Bardayan,[1] C. Boomershine,[1] K. Brandenburg,[3] C. Brune,[3] S. Coil,[1] M. Couder,[1] J. Derkin,[3] S. Dede,[1] R. Fang,[1] A. Fritsch,[4] A. Gula,[1] Gy. Gyürky,[5] B. Hackett,[6] G. Hamad,[3] Y. Jones-Alberty,[3] R. Kelmar,[1] K. Manukyan,[1] M. Matney,[1] J. McDonaugh,[1] Z. Meisel,[3] S. Moylan,[1] J. Nattress,[2] D. Odell,[3] P. O'Malley,[1] M. W. Paris,[7] D. Robertson,[1] Shahina,[1] N. Singh,[3] K. Smith,[8] M. S. Smith,[2] E. Stech,[1] W. Tan,[1] and M. Wiescher[1]

[1]*Department of Physics and Astronomy, University of Notre Dame, Notre Dame, Indiana 46556, USA*
[2]*Oak Ridge National Laboratory, Oak Ridge, Tennessee 37831, USA*
[3]*Department of Physics and Astronomy, Ohio University, Athens, Ohio 45701, USA*
[4]*Department of Physics, Gonzaga University, Spokane, Washington 99258, USA*
[5]*Institute for Nuclear Research (Atomki), P.O.B 51, H-4001 Debrecen, Hungary*
[6]*Department of Physics and Astronomy, University of Tennessee, Knoxville, Tennessee 37996, USA*
[7]*Theoretical Division, Los Alamos National Laboratory, Los Alamos, New Mexico 87545, USA*
[8]*Los Alamos National Laboratory, Los Alamos, New Mexico 87545, USA*

(Received 18 March 2023; revised 5 September 2023; accepted 17 January 2024; published 9 February 2024)

The cross section of the $^{13}C(\alpha, n)^{16}O$ reaction is needed for nuclear astrophysics and applications to a precision of 10% or better, yet inconsistencies among 50 years of experimental studies currently lead to an uncertainty of ≈15%. Using a state-of-the-art neutron detection array, we have performed a high resolution differential cross section study covering a broad energy range. These measurements result in a dramatic improvement in the extrapolation of the cross section to stellar energies potentially reducing the uncertainty to ≈5% and resolving long standing discrepancies in higher energy data.

DOI: 10.1103/PhysRevLett.132.062702

The $^{13}C(\alpha, n)^{16}O$ reaction, or its time reverse $^{16}O(n, \alpha)^{13}C$, is important for a wide range of applications in nuclear physics. In nuclear astrophysics, the low-energy cross section determines the neutron production in a variety of stellar environments and is critical for modeling the chemical evolution of our Universe. In asymptotic giant branch (AGB) stars, the mixing of hydrogen into the helium burning shell triggers the $^{12}C(p, \gamma)^{13}N(\beta^+\nu)^{13}C$ sequence producing ^{13}C to feed the $^{13}C(\alpha, n)^{16}O$ reaction. The strength of this neutron source depends on hydrodynamic intershell mixing conditions, the so-called carbon pocket, and the strength of the reaction. Thus, it determines the neutron flux for the slow-neutron-capture or *s* process, which is responsible for the synthesis of approximately half the heavy, naturally occurring, elements [1]. It is also necessary for modeling neutron production in AGB stars by comparing the abundance distribution of *s*-process elements [2]. At higher energies, it plays an important role in determining the neutron flux for intermediate neutron capture (*i* process) in carbon enhanced metal poor stars [3], where the neutron production occurs in a deep, convective, hot, environment in which ^{13}N is mixed into the hotter regions of the hydrogen burning shell before its decay, and the subsequent $^{13}C(\alpha, n)^{16}O$ reaction occurs at much higher temperatures [4,5].

In some large scale neutrino detector measurements, such as period 1 of the Kamioka Liquid Scintillator Antineutrino Detector (KamLAND), the $^{13}C(\alpha, n)^{16}O$ reaction is a main background source, competing with signals from geoneutrinos, in the determination of neutrino mixing $\nu_1 - \nu_2$ [6–8]. The reaction is induced by α particles released through the natural decay chains in impurities in the liquid scintillator material. Thus, the background depends on both actinide impurities and the neutron branching in the deexcitation channel. There are two ways the $^{13}C(\alpha, n)^{16}O$ reaction can mimic these interactions. First, through the production of high energy neutrons from the $^{13}C(\alpha, n_0)^{16}O$ reaction that inelastically scatters on ^{12}C producing a prompt γ ray followed by a neutron capture. Second, the $^{13}C(\alpha, n_1)^{16}O$ reaction [9,10] produces an $E0$ decay, $e+/e-$ followed by neutron capture, which is indistinguishable from inverse β decay. Therefore, experimentally determining the partial cross section to each of the individual final states is essential.

Additionally, neutron transport simulations play an important role in the nuclear energy sector. They are based on cross section evaluations like ENDF/B, where the $^{16}O(n, \alpha)^{13}C$ reaction is given high priority [11–13]. These simulations are necessary to estimate the flux of neutrons traversing from reactor or other neutron environments, to determine the energy distribution, calculate shielding and moderator requirements, and assess the lifetime of reactor fuel. Monte Carlo simulations of neutron transport are critical for studying the response of neutron detectors employed in low-, intermediate-, and high-energy physics as well as for estimating the activity induced in

different detectors by intense neutron fields. The latter is an important aspect for neutron dosimetry.

Past experimental studies have focused on reaction cross section measurements via detection of thermalized neutrons using "4π" moderator counters [14–18]. This measurement technique has the advantage of high detection efficiency, and, in principle, insensitivity to the angular distributions of the outgoing neutrons. However, it also has its drawbacks. With no sensitivity to outgoing neutron energy, backgrounds are more difficult to discriminate. Simulations have shown that when the moderator size is too small and the detector configuration is not optimized, the efficiency can be highly dependant on neutron energy and the neutron angular distribution [19]. The branching ratios to different final states and angular distributions are often unknown, and thus, the yields cannot be accurately converted to cross sections [20,21]. For these reasons, Harissopulos *et al.* [17] significantly underestimated their uncertainties, causing large inconsistencies to develop between the ENDF/B-VII.1 and ENDF/B-VIII.0 evaluations [12,22].

In order to resolve these discrepancies, new measurements were performed at the University of Notre Dame Nuclear Science Laboratory using the 5 MV Stable ion Accelerator for Nuclear Astrophysics [23]. Helium beams were produced over a laboratory energy range from $E_\alpha = 0.8$ to 6.5 MeV, with typical beam intensities of $\approx$10 $e\mu$A on target. The energy of the accelerator was calibrated using resonances in the $^{13}\mathrm{C}(\alpha, n)^{16}\mathrm{O}$ reaction that correspond to those observed in $n + {}^{16}\mathrm{O}$ time-of-flight measurements [24]. Targets were fabricated at the Institute for Nuclear Research (ATOMKI) in Debrecen, Hungary. Enriched (99%) ^{13}C powder was evaporated onto a 0.5 mm Ta backing, which also served as a beam stop, creating a thin layered reference target of 10.3(6) μg/cm^2. The target thickness was determined by measuring the energy loss over the narrow resonance in the $^{13}\mathrm{C}(\alpha, n)^{16}\mathrm{O}$ reaction at $E_\alpha = 1.05$ MeV. To mitigate deterioration from beam heating, the target backing was water-cooled throughout the experiment and the beam was rastered over the target area. A liquid-nitrogen cooled and electrically isolated copper pipe, biased to -300 V, was mounted in the target chamber to serve as both as a cold trap and electron suppressor.

The reference target was used to perform the majority of the measurements, accumulating $\approx$0.8 C of charge, and no deterioration was observed above the $\approx$5% level. A target of half this thickness was used to scan over narrow resonances in order to reduce the distortion from energy averaging effects. After $\approx$0.46 C of accumulated charge, the thin target was found to degrade by $\approx$15%. The targets were similar to those used by Ciani *et al.* [25].

The measurement of differential cross sections was accomplished using the Oak Ridge National Laboratory Deuterated Spectroscopic Array (ODeSA) [26], used previously in Refs. [9,27,28]. The array consisted of nine deuterated scintillators mounted on a swing arm, which was rotated to two different positions, with an offset of 7.5°, in order to map 18 point angular distributions between 0° and 157.5°. The response matrix for the ODeSA detectors [26] was measured at the Edwards Accelerator Laboratory at Ohio University using time-of-flight and the well-known $^9\mathrm{Be}(d, n)^{10}\mathrm{B}$ thick-target neutron yield [29], which was determined relative to measurements with a ^{235}U fission chamber [30]. In this way, direct current beams could be used, optimizing run times by way of higher beam intensities and simplified beam preparation. Neutron spectroscopy was accomplished by unfolding the light response spectra using the calibrated detector response matrix and an unfolding algorithm [31,32]. The data are provided in the Supplemental Material [33] and are shown in Fig. 1.

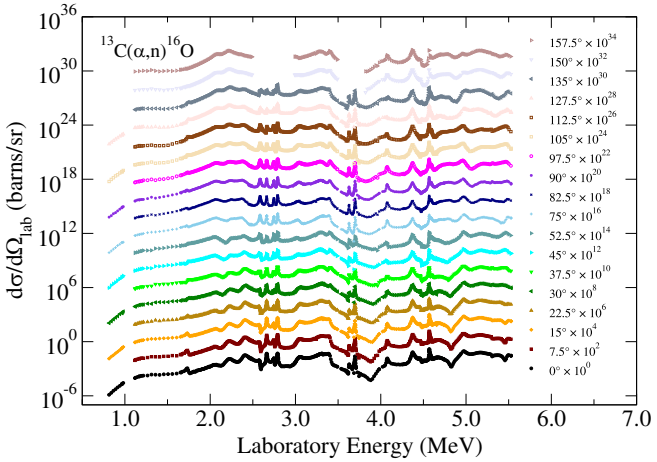

FIG. 1. The differential cross sections of the present work for the $^{13}\mathrm{C}(\alpha, n_0)^{16}\mathrm{O}$ reaction, where different angles of measurement have been scaled by the indicated multiplicative factor.

Because of the positive Q value of the $^{13}\mathrm{C}(\alpha, n_0)^{16}\mathrm{O}$ (+2.2 MeV) reaction, the above method was ideal, able to achieve better spectral resolution than time-of-flight for the target-to-detector distance of $\approx$63 cm [32]. The Ta backing produced very little background with peaks from the $^{19}\mathrm{F}(\alpha, n)^{22}\mathrm{Ne}$ reaction observed only at beam energies in excess of $E_\alpha \approx 3$ MeV. The large difference in Q value ($Q = -1.95$ MeV) ensured that the background was well separated, clearly distinguishable with the $\approx$6% energy resolution of the spectrum unfolding. However, this background source, and the unfolding resolution, prevented the extraction of excited state cross sections from the data.

The most significant corrections to the present data came from neutron scattering on the target backing, holder, and other beam components very close to the target. These corrections were simulated using MCNP6 [34], where a detailed model of the setup was created. These corrections were most significant at 0° and 90°, up to 30%, but were less than 10%, otherwise. The corrections were verified through comparison to previously measured neutron

TABLE I. Summary of systematic uncertainty estimates for the present measurements of the $^{13}C(\alpha, n)^{16}O$ cross section.

Systematic uncertainty contribution	%
Charge collection	3
Stopping power [38]	5
Intrinsic efficiency	5
MCNP/Geometric efficiency	10
Total	13

angular distributions on the thick target plateau of the $E_\alpha = 1.05$ MeV resonance [35] and angular distributions of $^7Li(p, n)^7Be$ reaction [36,37]. These corrections proved to be the most significant source of systematic uncertainty as summarized in Table I.

The main framework used for interpreting $^{13}C + \alpha$ and $^{16}O + n$ data over the resolved resonance region has been the R matrix [39,40]. A comprehensive analysis has been developed by the Los Alamos National Laboratory group for the ENDF/B evaluations [11,12] using the energy dependant analysis (EDA) code [41] and several other R-matrix studies have also been published [16,42–44]. The R-matrix parameters from the EDA fit were transformed into the Brune parametrization [45] and used as initial fit parameters for the AZURE2 [46,47] analysis described here. These parameter conversions have been tested previously in Thompson *et al.* [48].

Up to ≈2.6 MeV, the EDA parameters give a good reproduction of the present measurements owing to the previous measurements of Walton *et al.* [35], but at higher energies, the agreement worsens considerably because of the much more limited amount of data [49–51]. The recent measurements of Prusachenko *et al.* [52] provide 36 additional angular distributions, which have not yet been incorporated into the ENDF/B evaluation. The level of agreement between the present data and the EDA calculation is demonstrated by a comparison of the 0° cross section and two representative angular distributions in Fig. 2. The discrepancies highlight the improvement the present data can have on future evaluations.

In Febbraro *et al.* [9], it was confirmed that above ≈5 MeV the transitions to the excited states in ^{16}O quickly become significant contributors to the total reaction cross section. The present data give an improved mapping of the high energy $^{13}C(\alpha, n_0)^{16}O$ cross section up to 6.5 MeV. A Legendre fit was used to integrate the differential data to compare with the reaction cross section data of Brandenburg *et al.* [53] as shown in Fig. 3. The Brandenburg *et al.* [53] measurements should be more accurate than previous measurements as the efficiency of the detector was designed to minimize its sensitivity to neutron energy and angular distribution. Over the region where only the ground state transition is energetically accessible, the present data are ≈15% higher than those of Brandenburg *et al.* [53], 10% higher than those of Febbraro *et al.* [9], and ≈15% lower than those of Prusachenko *et al.* [52], in good agreement when these systematic uncertainties are considered. The data of Prusachenko *et al.* [52] do show some differences in their energy dependence, but this is likely due to energy resolution effects resulting from their thicker target.

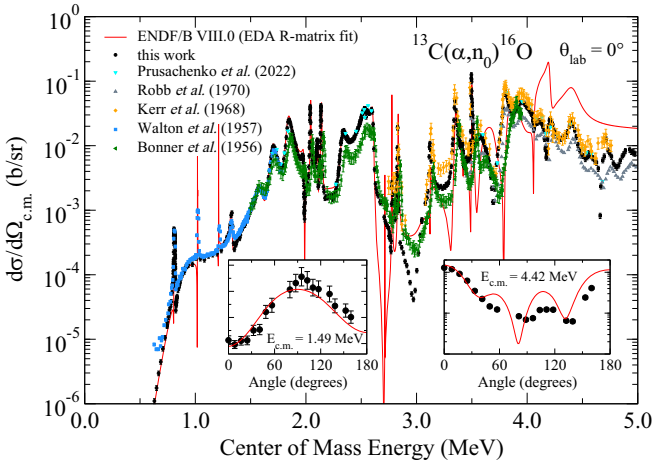

FIG. 2. Comparison of the present measurements with those of Refs. [35,49–52] and the R-matrix cross section from the ENDF/B VIII.0 evaluation [12] at $\theta_{lab} = 0°$ and two example angular distributions from this work.

Recently, measurements have been extended to lower energies [54,55], now directly overlapping a portion of the Gamow window for helium burning temperatures. Even so, an extrapolation of the cross section is still required to cover the full range of astrophysical interest. Using the R matrix, the uncertainty can be more fully characterized as the framework provides the means for combining direct measurements with asymptotic normalization coefficients

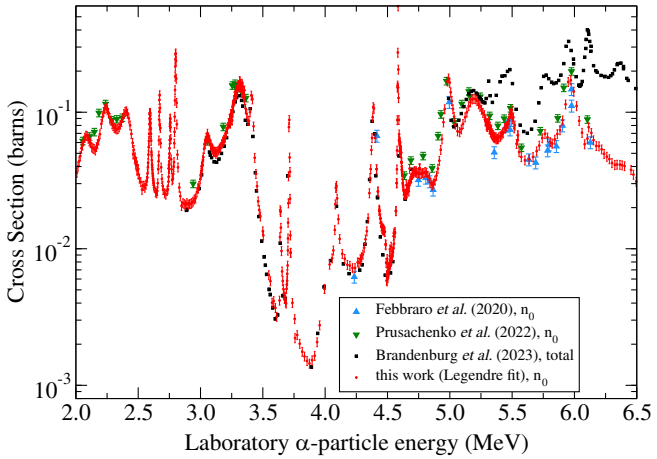

FIG. 3. Comparison of the present $^{13}C(\alpha, n_0)^{16}O$ data and that of Refs. [9,52] to the $^{13}C(\alpha, n)^{16}O$ data of Brandenburg *et al.* [53]. The data above $E_\alpha \approx 5$ MeV indicate strong contributions from excited state transitions.

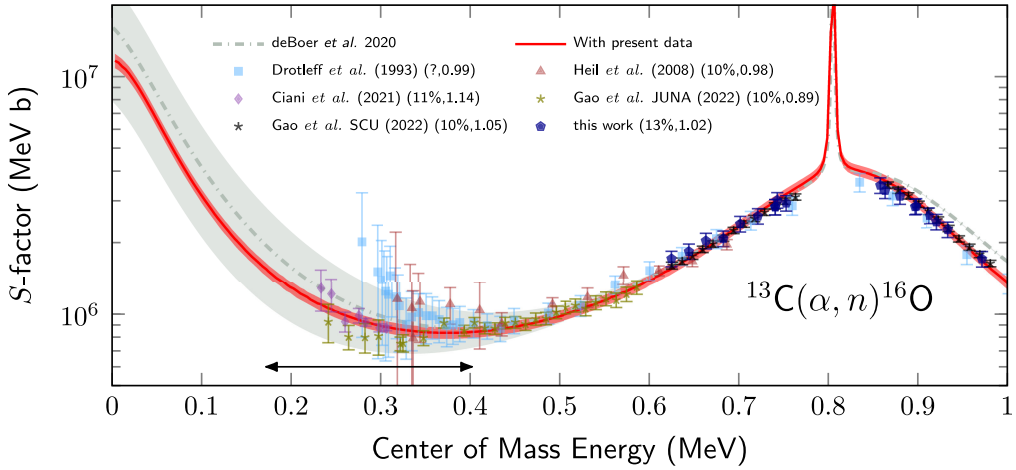

FIG. 4. S factor for the $^{13}C(\alpha,n)^{16}O$ reaction at low energies. The shaded gray region indicates the uncertainty estimated by deBoer *et al.* [61]. The red region represents the 16% and 84% confidence limits obtained from the BRICK analysis with the present data. The percentages following each data set indicate the systematic uncertainty of that work. The data have been scaled according to the normalization factors obtained from the fit as given in the Supplemental Material [33]. The arrow indicates the Gamow energy range for $T = 0.2$ GK.

(ANC) from α-transfer measurements. This has become particularly important given the advances in ANC determinations [56–59] and the Trojan horse method [60].

To demonstrate the effect that this data has on the extrapolation of the S factor, the uncertainty range estimated in deBoer *et al.* [61] is indicated in Fig. 4. This uncertainty comes from the systematic differences in the absolute cross sections of Refs. [17,18] compared to those of Refs. [14–16] and differences in extrapolation techniques. The data of the present work and that of Gao *et al.* [55] both strongly favor an absolute cross section consistent with the measurements of Refs. [14–16]. Thus, the assertion is made that this source of systematic uncertainty has been greatly reduced.

An R-matrix fit was performed that utilized the consistent data of Refs. [15,16,54,55] up to $E_{\mathrm{c.m.}} = 2.6$ MeV as well as the $^{16}O(n,\mathrm{total})$ data of Refs. [24,62]. A Bayesian uncertainty analysis was then performed using the code BRICK [63]. In addition to providing more detailed information about the parameter and cross section uncertainties through the posterior probability distributions, this methodology provided a natural way for the sub-Coulomb ANC and its uncertainty for the near threshold state [59] to be included directly as a prior. It should be noted that, as found in Gao *et al.* [55], a consistent value for the ANC is found even if a uniform prior is assumed. The systematic uncertainties of each data set are also considered assuming Gaussian priors and that no correlations exist. The resulting best fit gives an ≈10% uncertainty over the Gamow energy range. This analysis is similar to that performed in Ciani *et al.* [54].

To demonstrate their affect, the new data were then introduced into the fit. It should be noted that while the angle integrated cross section, obtained through a Legendre fit of the angular distributions has been shown for comparison in Fig. 4, the actual fit used the differential data directly. This resulted in a further reduction in the S-factor uncertainty to ≈5% over the Gamow energy range. The two fits are largely consistent with one another over the Gamow energy range, indicating the consistency of the present data set with previous ones, but the reduced uncertainty demonstrates the significant additional constraint that the differential cross section data have on the R-matrix model. The differential data are especially significant given the presence of broad, overlapping, resonances that produce additional angle dependent interference. This highlights the very complementary nature of extremely low-energy angle-integrated measurements, that require high detection efficiency, with high resolution differential measurements, that can only be made where the cross section is larger. It must be emphasized, however, that this fit only represents the potential effect of the present data and that a full evaluation of all of the data must still be made to fully characterize the uncertainties. Further details on the fit can be found in the Supplemental Material [33].

The $^{13}C(\alpha,n)^{16}O$ reaction is one of the main sources of neutrons for s-process nucleosynthesis, it is a significant background in many kiloton-scale, low-event-rate, neutrino and dark matter detectors, and its inverse $^{16}O(n,\alpha)^{13}C$ is needed to model neutron induced α-particle production for a variety of applications. The realization of additional sources of uncertainty in past measurements has prompted new experimental techniques. In this work, we report new high-resolution measurements, in both energy and angle, for the $^{13}C(\alpha,n_0)^{16}O$ cross section, using the state-of-the-art ODeSA array, resulting in 714 distinct angular distributions that encompass the energy ranges applicable for many applications. To demonstrate the effect of these new

data on the extrapolation of the low-energy S factor, R-matrix fits were combined with Bayesian uncertainty estimation, which indicate the potential for a substantial reduction in the uncertainty over the entire Gamow energy range.

This research utilized resources from the Notre Dame Center for Research Computing. Researchers at the University of Notre Dame were funded by the National Science Foundation through Grant No. PHY-2011890 (University of Notre Dame Nuclear Science Laboratory) and Grant No. PHY-1430152 (the Joint Institute for Nuclear Astrophysics—Center for the Evolution of the Elements) and under Grant No. OISE-1927130 (IReNA). This material is based upon work supported by the U.S. Department of Energy, Office of Science, Office of Nuclear Physics, under Award No. DE-AC05-00OR22725. LANL researchers are supported by the U.S. Department of Energy, through the Los Alamos National Laboratory, operated by Triad National Security, LLC, for the National Nuclear Security Administration of U.S. Department of Energy (Contract No. 89233218CNA000001) and by the Office of Science, Office of Nuclear Physics, under the Nuclear Data InterAgency Working Group Research Program.

*rdeboer1@nd.edu

[1] O. Straniero, R. Gallino, and S. Cristallo, *s* process in low-mass asymptotic giant branch stars, Nucl. Phys. **A777**, 311 (2006), special Issue on Nuclear Astrophysics.

[2] S. Bisterzo, C. Travaglio, M. Wiescher, F. Käppeler, and R. Gallino, Galactic chemical evolution: The impact of the ^{13}C-pocket structure on the *s*-process distribution, Astrophys. J. **835**, 97 (2017).

[3] D. Carollo, K. Freeman, T. C. Beers, V. M. Placco, J. Tumlinson, and S. L. Martell, Carbon-enhanced metal-poor stars: CEMP-*s* and CEMP-no subclasses in the halo system of the Milky Way, Astrophys. J. **788**, 180 (2014).

[4] O. Clarkson, F. Herwig, and M. Pignatari, Pop III *i*-process nucleosynthesis and the elemental abundances of SMSS J0313-6708 and the most iron-poor stars, Mon. Not. R. Astron. Soc. **474**, L37 (2017).

[5] O. Clarkson, F. Herwig, and M. Pignatari, Erratum: Pop III *i*-process nucleosynthesis and the elemental abundances of SMSS J0313-6708 the most iron-poor stars, Mon. Not. R. Astron. Soc. **488**, 222 (2019).

[6] A. Gando *et al.* (The KamLAND Collaboration), Constraints on θ_{13} from a three-flavor oscillation analysis of reactor antineutrinos at KamLAND, Phys. Rev. D **83**, 052002 (2011).

[7] K. Ichimura and Y. Minekawa, Background study for the KamLAND reactor neutrino experiment, J. Phys. Conf. Ser. **120**, 052034 (2008).

[8] S. Abe *et al.* (The KamLAND Collaboration), Abundances of uranium and thorium elements in earth estimated by geoneutrino spectroscopy, Geophys. Res. Lett. **49**, e2022GL099566 (2022).

[9] M. Febbraro *et al.*, New $^{13}\mathrm{C}(\alpha,n)^{16}\mathrm{O}$ cross section with implications for neutrino mixing and geoneutrino measurements, Phys. Rev. Lett. **125**, 062501 (2020).

[10] R. J. deBoer, A. Gula, M. Febbraro, K. Brandenburg, C. R. Brune, J. Görres, G. Gyürky, R. Kelmar, K. Manukyan, Z. Meisel, D. Odell, M. T. Pigni, Shahina, E. Stech, W. Tan, and M. Wiescher, First near-threshold measurements of the $^{13}\mathrm{C}(\alpha,n_1)^{16}\mathrm{O}$ reaction for low-background-environment characterization, Phys. Rev. C **106**, 055808 (2022).

[11] M. Chadwick *et al.*, Cielo Collaboration summary results: International evaluations of neutron reactions on uranium, plutonium, iron, oxygen and hydrogen, Nucl. Data Sheets **148**, 189 (2018), Special Issue on Nuclear Reaction Data.

[12] D. Brown *et al.*, ENDF/B-VIII.0: The 8th major release of the nuclear reaction data library with CIELO-project cross sections, new standards and thermal scattering data, Nucl. Data Sheets **148**, 1 (2018), Special Issue on Nuclear Reaction Data.

[13] C. E. Romano, D. A. Brown, S. Croft, A. Favali, L. Nakae, M. T. Pigni, M. S. Smith, S. Skutnik, W. Wieselquist, and M. Zerkle, (α,n) nuclear data scoping study, 10.2172/1771892 (2020).

[14] J. K. Bair and F. X. Haas, Total neutron yield from the reactions $^{13}\mathrm{C}(\alpha,n)^{16}\mathrm{O}$ and $^{17,18}\mathrm{O}(\alpha,n)^{20,21}\mathrm{Ne}$, Phys. Rev. C **7**, 1356 (1973).

[15] H. W. Drotleff, A. Denker, H. Knee, M. Soine, G. Wolf, J. W. Hammer, U. Greife, C. Rolfs, and H. P. Trautvetter, Reaction rates of the *s*-process neutron sources $^{22}\mathrm{N}(\alpha,n)^{25}\mathrm{Mg}$ and $^{13}\mathrm{C}(\alpha,n)^{16}\mathrm{O}$, Astrophys. J. **414**, 735 (1993).

[16] M. Heil, R. Detwiler, R. E. Azuma, A. Couture, J. Daly, J. Görres, F. Käppeler, R. Reifarth, P. Tischhauser, C. Ugalde, and M. Wiescher, The $^{13}\mathrm{C}(\alpha,n)$ reaction and its role as a neutron source for the *s* process, Phys. Rev. C **78**, 025803 (2008).

[17] S. Harissopulos, H. W. Becker, J. W. Hammer, A. Lagoyannis, C. Rolfs, and F. Strieder, Cross section of the $^{13}\mathrm{C}(\alpha,n)^{16}\mathrm{O}$ reaction: A background for the measurement of geo-neutrinos, Phys. Rev. C **72**, 062801(R) (2005).

[18] S. Kellogg, R. Vogelaar, and R. Kavanagh, $^{13}\mathrm{C}(\alpha,n)$ and $^{14}\mathrm{C}(p,n)$: Astrophysical neutron sources and sinks, Bull. Am. Phys. Soc. **34**, 1192 (1989).

[19] Y.-T. Li, W.-P. Lin, B.-S. Gao, H. Chen, H. Huang, Y. Huang, T.-Y. Jiao, K.-A. Li, X.-D. Tang, X.-Y. Wang, X. Fang, H.-X. Huang, J. Ren, L.-H. Ru, X.-C. Ruan, N.-T. Zhang, and Z.-C. Zhang, Development of a low-background neutron detector array, Nucl. Sci. Tech. **33**, 41 (2022).

[20] W. A. Peters, Comment on "Cross section of the $^{13}\mathrm{C}(\alpha,n)^{16}\mathrm{O}$ reaction: A background for the measurement of geo-neutrinos", Phys. Rev. C **96**, 029801 (2017).

[21] P. Mohr, Revised cross section of the $^{13}\mathrm{C}(\alpha,n)^{16}\mathrm{O}$ reaction between 5 and 8 MeV, Phys. Rev. C **97**, 064613 (2018).

[22] M. Chadwick *et al.*, ENDF/B-VII.1 Nuclear data for science and technology: Cross sections, covariances, fission product yields and decay data, Nucl. Data Sheets **112**, 2887 (2011), Special Issue on ENDF/B-VII.1 Library.

[23] A. Aprahamian, P. Collon, and M. Wiescher, The nuclear science laboratory at the university of Notre Dame, Nucl. Phys. News **24**, 5 (2014).

[24] S. Cierjacks, F. Hinterberger, G. Schmalz, D. Erbe, P. Rossen, and B. Leugers, High precision time-of-flight measurements of neutron resonance energies in carbon and oxygen between 3 and 30 MeV, Nucl. Instrum. Methods **169**, 185 (1980).

[25] G. F. Ciani *et al.*, A new approach to monitor ^{13}C-targets degradation *in situ* for $^{13}C(\alpha,n)^{16}O$ cross-section measurements at LUNA, Eur. Phys. J. A **56**, 75 (2020).

[26] M. Febbraro *et al.*, The ORNL deuterated spectroscopic array—ODeSA, Nucl. Instrum. Methods Phys. Res., Sect. A **946**, 162668 (2019).

[27] Q. Liu *et al.*, Measurement of the $^{10}B(\alpha,n_0)^{13}N$ cross section for $2.2 < E_\alpha < 4.9$ MeV and its application as a diagnostic at the National Ignition Facility, Phys. Rev. C **100**, 034601 (2019).

[28] Q. Liu *et al.*, Low-energy cross-section measurement of the $^{10}B(\alpha,n)^{13}N$ reaction and its impact on neutron production in first-generation stars, Phys. Rev. C **101**, 025808 (2020).

[29] T. N. Massey, D. K. Jacobs, S. I. Al-Quraishi, S. M. Grimes, C. E. Brient, W. B. Howard, and J. C. Yanch, Study of the $Be(p,n)$ and $Be(d,n)$ source reactions, J. Nucl. Sci. Technol. **39**, 677 (2002).

[30] J. W. Meadows, The $^{9}Be(d,n)$ thick-target neutron spectra for deuteron energies between 2.6 and 7.0 MeV, Nucl. Instrum. Methods Phys. Res., Sect. A **324**, 239 (1993).

[31] M. Febbraro, C. Lawrence, H. Zhu, B. Pierson, R. Torres-Isea, F. Becchetti, J. Kolata, and J. Riggins, Deuterated scintillators and their application to neutron spectroscopy, Nucl. Instrum. Methods Phys. Res., Sect. A **784**, 184 (2015), symposium on Radiation Measurements and Applications 2014 (SORMA XV).

[32] M. Febbraro *et al.*, Performance of neutron spectrum unfolding using deuterated liquid scintillator, Nucl. Instrum. Methods Phys. Res., Sect. A **989**, 164824 (2021).

[33] See Supplemental Material at http://link.aps.org/supplemental/10.1103/PhysRevLett.132.062702 for the tabulated experimental data, AZURE2 input file, and normalizations of the fitted data.

[34] T. Goorley *et al.*, Features of MCNP6 , Ann. Nucl. Energy **87**, 772 (2016).

[35] R. B. Walton, J. D. Clement, and F. Boreli, Interaction of neutrons with oxygen and a study of the $C^{13}(\alpha,n)O^{16}$ reaction, Phys. Rev. **107**, 1065 (1957).

[36] S. Elbakr, I. Van Heerden, W. McDonald, and G. Neilson, Measurements of neutron angular distributions from the $^{7}Li(p,n)^{7}Be$ reaction, Nucl. Instrum. Methods **105**, 519 (1972).

[37] C. A. Burke, M. T. Lunnon, and H. W. Lefevre, $^{7}Li(p,n_0)^{7}Be$ angular distributions to $E_p = 3.8$ MeV, Phys. Rev. C **10**, 1299 (1974).

[38] J. F. Ziegler, M. D. Ziegler, and J. P. Biersack, SRIM—The stopping and range of ions in matter (2010), Nucl. Instrum. Methods Phys. Res., Sect. B **268**, 1818 (2010).

[39] A. M. Lane and R. G. Thomas, *R*-matrix theory of nuclear reactions, Rev. Mod. Phys. **30**, 257 (1958).

[40] P. Descouvemont and D. Baye, The *R*-matrix theory, Rep. Prog. Phys. **73**, 036301 (2010).

[41] D. Dodder, G. Hale, and K. Witte, The energy dependant analysis code, Technical Report, Los Alamos National, 1972.

[42] R. Sayer, L. Leal, N. Larson, R. Spencer, and R. Wright, *R*-matrix evaluation of ^{16}O neutron cross sections up to 6.3 MeV, Nucl. Sci. Technol. **39**, 88 (2002).

[43] L. Leal, E. Ivanov, G. Noguere, A. Plompen, and S. Kopecky, Resonance parameter and covariance evaluation for ^{16}O up to 6 MeV, Eur. J. Nucl. Sci. Technol. **2**, 43 (2016).

[44] S. Chakraborty, A. Mukherjee, and S. Roy, *R*-matrix analyses of $^{16}O(n,n)$ scattering and $^{13}C(\alpha,n)$ reaction at astrophysical energies relevant to low-mass AGB stars, Int. J. Mod. Phys. E **28**, 1950076 (2019).

[45] C. R. Brune, Alternative parametrization of *R*-matrix theory, Phys. Rev. C **66**, 044611 (2002).

[46] R. E. Azuma, E. Uberseder, E. C. Simpson, C. R. Brune, H. Costantini, R. J. de Boer, J. Görres, M. Heil, P. J. LeBlanc, C. Ugalde, and M. Wiescher, AZURE: An *R*-matrix code for nuclear astrophysics, Phys. Rev. C **81**, 045805 (2010).

[47] E. Uberseder and R. J. deBoer, AZURE2 User Manual (2015).

[48] I. Thompson, R. deBoer, P. Dimitriou, S. Kunieda, M. Pigni, G. Arbanas, H. Leeb, T. Srdinko, G. Hale, P. Tamagno, and P. Archier, Verification of *R*-matrix calculations for charged-particle reactions in the resolved resonance region for the ^{7}Be system, Eur. Phys. J. A **55**, 92 (2019).

[49] T. W. Bonner, A. A. Kraus, J. B. Marion, and J. P. Schiffer, Neutrons and gamma rays from the alpha-particle bombardment of Be^{9}, B^{10}, B^{11}, C^{13}, and O^{18}, Phys. Rev. **102**, 1348 (1956).

[50] A. Robb, W. Schier, and E. Sheldon, Spin and parity assignments for ^{17}O levels from the $^{13}C(\alpha,n)^{16}O_{g.s.}$ reaction, Nucl. Phys. **A147**, 423 (1970).

[51] G. W. Kerr, J. M. Morris, and J. R. Risser, Energy levels of ^{17}O from $^{13}C(\alpha,\alpha_0)^{13}C$ and $^{13}C(\alpha,n)^{16}O$, Nucl. Phys. **A110**, 637 (1968).

[52] P. S. Prusachenko, T. L. Bobrovsky, I. P. Bondarenko, M. V. Bokhovko, A. F. Gurbich, and V. V. Ketlerov, Measurement of the cross section for the $^{13}C(\alpha,n)^{16}O$ reaction and determination of the cross section for the $^{16}O(n,\alpha)^{13}C$ reaction, Phys. Rev. C **105**, 024612 (2022).

[53] K. Brandenburg, G. Hamad, Z. Meisel, C. R. Brune, D. E. Carter, R. deBoer, J. Derkin, C. Feathers, D. Ingram, Y. Jones-Alberty, B. Kenady, T. N. Massey, M. Saxena, D. Soltesza, S. K. Subedi, A. V. Voinov, J. Warren, and M. Wiescher, Measurements of the $^{13}C(\alpha,n)^{16}O$ cross section up to $E_\alpha = 8$ MeV, Phys. Rev. C **108**, L061601 (2023).

[54] G. F. Ciani *et al.* (LUNA Collaboration), Direct measurement of the $^{13}C(\alpha,n)^{16}O$ cross section into the *s*-process Gamow peak, Phys. Rev. Lett. **127**, 152701 (2021).

[55] B. Gao *et al.* (JUNA Collaboration), Deep underground laboratory measurement of $^{13}C(\alpha,n)^{16}O$ in the Gamow windows of the *s* and *i* processes, Phys. Rev. Lett. **129**, 132701 (2022).

[56] S. Y. Mezhevych, A. T. Rudchik, A. A. Rudchik, O. A. Ponkratenko, N. Keeley, K. W. Kemper, M. Mazzocco, K. Rusek, and S. B. Sakuta, Cluster structure of ^{17}O, Phys. Rev. C **95**, 034607 (2017).

[57] M. G. Pellegriti, F. Hammache, P. Roussel, L. Audouin, D. Beaumel, P. Descouvemont, S. Fortier, L. Gaudefroy, J. Kiener, A. Lefebvre-Schuhl, M. Stanoiu, V. Tatischeff, and M. Vilmay, Indirect study of the $^{13}C(\alpha,n)^{16}O$ reaction via the $^{13}C(^{7}Li,t)^{17}O$ transfer reaction, Phys. Rev. C **77**, 042801 (R) (2008).

[58] B. Guo *et al.*, New determination of the $^{13}c(\alpha, n)^{16}o$ reaction rate and its influence on the *s*-process nucleosynthesis in the AGB stars, Astrophys. J. **756**, 193 (2012).

[59] M. L. Avila, G. V. Rogachev, E. Koshchiy, L. T. Baby, J. Belarge, K. W. Kemper, A. N. Kuchera, and D. Santiago-Gonzalez, New measurement of the α asymptotic normalization coefficient of the $1/2^+$ state in ^{17}O at 6.356 MeV that dominates the $^{13}C(\alpha, n)^{16}O$ reaction rate at temperatures relevant for the *s* process, Phys. Rev. C **91**, 048801 (2015).

[60] M. La Cognata, C. Spitaleri, O. Trippella, G. G. Kiss, G. V. Rogachev, A. M. Mukhamedzhanov, M. Avila, G. L. Guardo, E. Koshchiy, A. Kuchera, L. Lamia, S. M. R. Puglia, S. Romano, D. Santiago, and R. Spartà, On the measurement of the $^{13}C(\alpha, n)^{16}O$ *S*-factor at negative energies and its influence on the *s*-process, Astrophys. J. **777**, 143 (2013).

[61] R. J. deBoer, C. R. Brune, M. Febrarro, J. Görres, I. J. Thompson, and M. Wiescher, Sensitivity of the $^{13}C(\alpha, n)^{16}O$ *S* factor to the uncertainty in the level parameters of the near-threshold state, Phys. Rev. C **101**, 045802 (2020).

[62] J. L. Fowler, C. H. Johnson, and R. M. Feezel, Level structure of ^{17}O from neutron total cross sections, Phys. Rev. C **8**, 545 (1973).

[63] D. Odell, C. R. Brune, D. R. Phillips, R. J. deBoer, and S. N. Paneru, Performing Bayesian analyses with AZURE2 using BRICK: An application to the ^{7}Be system, Front. Phys. **10**, 888476 (2022).